SUPPLEMENTARY MATERIALS AND METHODS

BCCAS

Anaesthesia was achieved using isoflurane in a 70:30 nitrous oxide:oxygen mixture and core body temperature was maintained at 37 ± 0.2 °C with an automated rectal probe and heat blanket. A midline incision was made in the neck, and a carotid artery was carefully exposed. Hypoperfusion was induced by winding a custom ordered, non-magnetic, surgical grade microcoil (160 μm inner diameter, Shannon Coiled Springs Microcoil, Limerick, Ireland) around one of the carotid arteries. The sham procedure was performed with a larger diameter microcoil (500 μm) that did not constrict the vessel. The muscle and glands were guided back into place and local anaesthetic was applied to the sutured wound prior to recovery. Twenty- four hours later, the same procedure was repeated on the other carotid artery. This delay represents an important refinement that does not result in higher mortality when using the smaller sized microcoils. Regular diet was placed on the floor of the cage to assist with feeding. In the BCCAS model, hypoperfusion was induced by winding a custom ordered, nonmagnetic, surgical grade microcoil (160 μm inner diameter; Shannon Coiled Springs Microcoil, Limerick, Ireland) around one of the common carotid arteries. The muscles and glands were guided back into place, and local anesthetic was applied to the sutured wound before recovery. Twenty-four hours later, the same procedure was repeated on the other common carotid artery. This delay represents an important refinement that does not result in higher mortality when using the smaller sized microcoils.

MCAO

In the MCAO model, hypoperfusion was induced as described previously (http://precedings.nature.com/documents/3492/version/2). Briefly, after closing the left common carotid artery (CCA) and left external carotid artery (ECA) a microvascular clip was put on the left internal carotid artery (ICA) and a small incision was made on the CCA. A nylon filament (7019PK5Re, Doccol Corp, Redlands, California, USA) was introduced over CCA and ICA to occlude the origin of middle cerebral artery (MCA) and fixed with a suture around the ICA. After 60 minutes, the filament was removed causing immediate reperfusion. Afterwards the suture on the ICA was closed. This type of MCAO surgery results in permanent occlusion of left CCA, ECA and ICA.

MRI measurements

Anaesthesia was again achieved using isoflurane as per above, and body temperature and respiration rate were monitored with MRI compatible equipment (Small Animal Instruments, Inc., Stony Brook, NY).

Cerebral blood flow and angiographies

CBF and angiography were measured on a 7 T Pharmascan using Paravision 5.1 software (Bruker BioSpin, Ettlingen, Germany). For the CBF measurement, radio frequency transmission was achieved with a 72 mm diameter quadrature resonator actively decoupled to a mouse quadrature surface coil used for reception (Bruker BioSpin, Ettlingen, Germany). A single slice (1 mm) flow-sensitive alternating inversion recovery (FAIR) sequence with a rapid acquisition with relaxation enhancement (RARE) readout was used (repetition time (TR)/recovery time/echo spacing (ΔTE)/effective echo time (TEeff): 12 000/10 000/7.2/35.9 ms, respectively, 16 inversion times (35-1500 ms), RARE factor: 32, inversion slice thickness: 4 mm, 180° hyperbolic secant (sech80) inversion pulse (20 ms), field of view (FOV): 25.6 mm2, matrix: 128 x 64 enlarged by partial fourier transform to 128 x 128, resolution: 200 µm2, 12 min). For angiography measurements, a 20 mm diameter quadrature volume coil (RAPID Biomedical, Rimpar, Germany) was used for radio frequency transmission and reception and a 3D time of light (TOF) sequence was used (TR/TE: 15/2.5 ms, α: 20 ˚, FOV: 25 mm3, resolution: 98 x 130 x 196 µm3 zero-filled to 98 µm3, 6 min). Spectroscopy, T2 weighted and MR spectra were acquired on a 7 T Biospec with a cryogenically cooled transmit/receive surface coil and Paravision 6.0 software (Bruker BioSpin, Ettlingen, Germany).

A 2D RARE T2 sequence was used for anatomical images (TR/ΔTE/TEeff: 3100/11/33 ms, RARE factor: 8, 29 consecutive slices, slice thickness 0.45 mm, FOV: (16.2 mm)2, resolution: 100 µm2, NA: 2, 2 min 4 s). A stimulated echo acquisition mode (STEAM) sequence was used for spectroscopy following local shimming (MAPSHIM) across a cubic 8 mm3 voxel placed in the striatum (TR/TE/mixing time: 2500 ms/3 ms/10 ms, number of averages (NA): 256, VAPOR water suppression, 10 min 40 s).

MRI Data Analysis

CBF maps were calculated using the Perfusion ASL macro in Paravision 5.1 software via the T1 method using a blood T1 value of 2100 ms and a brain blood partition coefficient of 0.89 mL/g [1,2]. Analysis of the CBF values were done using a custom written Matlab toolbox for nonlinear atlas registration [3] was used to select the CBF slice from the volume and coregister the CBF on the T2 images. Finally T2 and CBF images were transformed into the

Allen brain atlas space and the atlas based CBF-values were extracted for all correlating Allen brain atlas structures in both hemispheres. (Release 2013a (MathWorks, Natick, MA, USA) script extracted the CBF maps from Paravision, and used atlas registration and coregistration of CBF maps in the atlas space for striatum and prefrontal cortex). The resulting CBF values were expressed in mL/min/100g.

Tissue preparation and staining procedures

At the conclusion of the experiments, mice were deeply anaesthetized with ketamine and xylazine and perfused through the heart with physiological saline followed by 4% paraformaldehyde, Alexa Fluor® 680 conjugate of WGA, Termofisher, W32465, 3% Gelatin (Sigma-Aldrich, G1890), 1% low melting agarose (Sigma Aldrich A4018) and 0.1% Evans Blue (Sigma Aldrich E2129). Whole brains were scanned with Li-cor (Li-Cor Odyssey-CLx). Subsequently, the brains were post-fixed for 24 hours in 4% PFA, and cryoprotected in 30% sucrose solution before being snap frozen in -40 ºC methylbutane. Tissue was sectioned to 50 µm and stored in cryo-protective solution (1 part ethylene glycol, 1 part glycerine and 2 parts phosphate buffered saline (PBS)) at -20 ºC.

Retina histology

Imunohistochemistochemical analysis of retinal sagittal sections was performed as previously described (Crespo-Garcia et al. PLOS ONE 2018). In short, after fixation of the eyes in 4% PFA and embedding in paraffin, 5um thin sections were stained for H/E, or GFAP (Z0334, DAKO, Hamburg, Germany) or CTBP2 (ab128871, Abcam, Cambridge GB) at 4°C overnight. Subsequently the sections were incubated with fluorescence conjugated secondary antibodies for 1h at RT and nuclei were counterstained with DAPI (Sigma, Taufkirchen, Germany). Images were digitalized using a Zeiss Axio Imager microscope and Zen-Lite 2012 software (Zeiss, Jena, Germany)

References

1. Leithner C, Müller S, Füchtemeier M, et al. Determination of the brain-blood partition coefficient for water in mice using MRI. *J Cereb Blood Flow Metab* 2010; 30: 1821–1824.

2. Dobre MC, Uğurbil K, Marjanska M. Determination of blood longitudinal relaxation time (T1) at high magnetic field strengths. *Magn Reson Imaging* 2007; 25: 733–735.

3. Koch S, Mueller S, Foddis M, et al. Atlas registration for edema-corrected MRI lesion volume in mouse stroke models. *J Cereb Blood Flow Metab* 2017; 271678X17726635.

Legends supplementary figures and tables

Fig S1

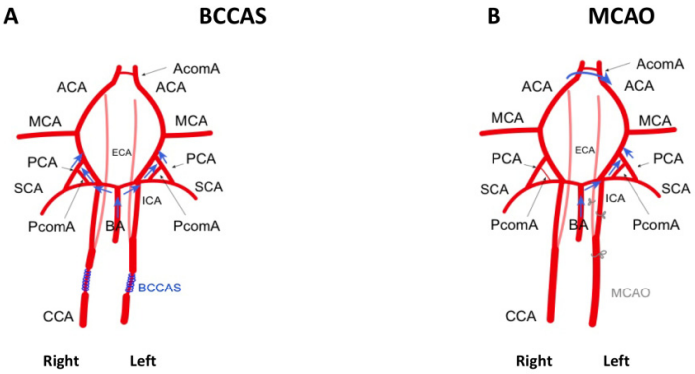

FigS1

MCAO and BCCAS models with surgical key features and collateral blood flow during acute ischemia. The blue arrows indicate the direction of the collateral blood flow following the surgery. **A**. Basilar artery (BA) → superior cerebellar artery (SCA) → posterior communicating artery (PcomA) → posterior cerebral artery (PCA). **B.** Basilar artery (BA) → left superior cerebellar artery (SCA) → left posterior communicating artery (PcomA) → left posterior cerebral artery (PCA) and right anterior cerebral artery (ACA) → anterior communicating artery (AcomA) → left anterior cerebral artery (ACA). CCA, common carotid artery, BA, basilar artery, ICA, internal carotid artery, OA, ophthalmic artery.

Fig S2

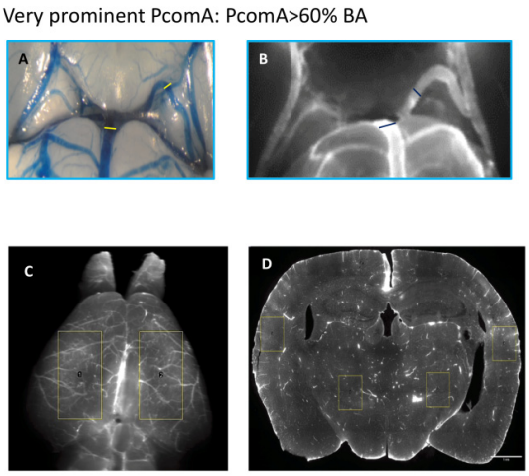

FigS2

A-B exemple of very prominent PcomA, based on the PcomA/BA diameter ratio measurements both with Evans Blue and WGA stainings. **C-D** Angiotool analysis of microvessel density, average length and anastomoses at the superficial leptomeningeal and cortical and deep gray striatal level. Leptomeningeal and deep microvessels during hypoperfusion. Region of interest has been always kept the same, both in terms of dimensions and brain regions in both hemispheres. Scale bar = 1mm.

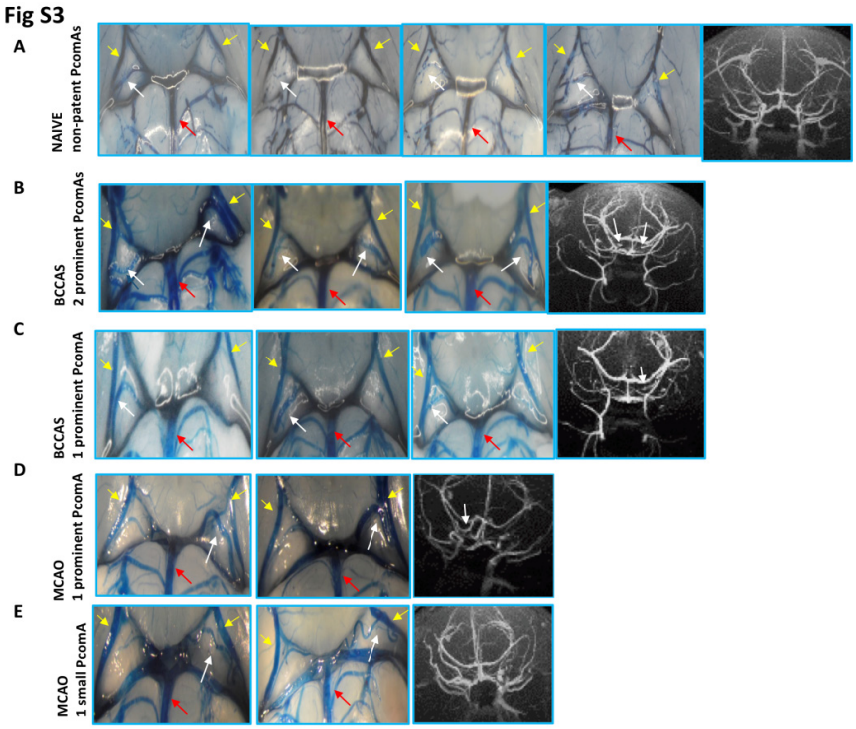

FigS3

PcomAs in naive, BCCAS and MCAO mice. In the absence of a pressure gradient in the Circle of Willis, PcomAs (white arrows) are not recruited and appear hypoplstic and subtle, not detectable on MRA. Analogously, basilar artery (BA, red arrow) and PCA (yellow arrows), PcomA affluents and effluents, respectively, display a small diameter (**A**). By contrast, during ischemia, PcomAs become patent, progressively more prominent, and clearly detectable on MRA (**B-D, MRI,** white arrows). **A** Naïve mice, displaying none or non-patent PcomAs. **B-C** BCCAS mice 7 days post-surgery, displaying 2 and 1 prominent PcomAs and BA with increased diameter. **D-E** MCAO mice, 7 wks post-surgery displaying prominent and small left PcomAs. **E** MCAO mice with very subtle PcomAs and markedly increased tortuosity on the left side, barely detectable on the MRA

Fig S4

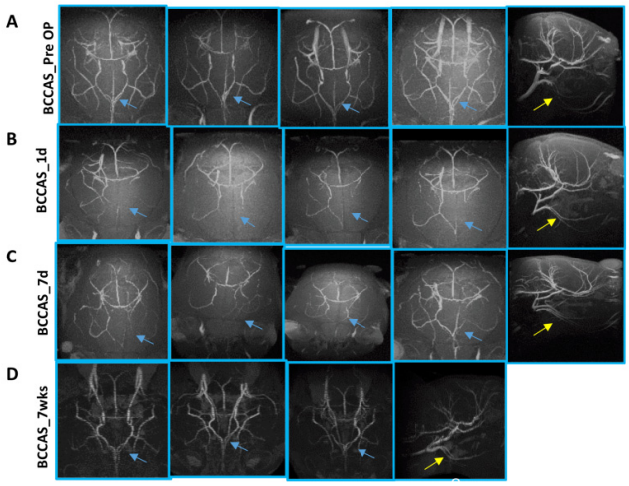

FigS4

BCCAS MRA showing Circle of Willis and ECA retrograde flow at different time points: pre-surgery, 1 day, 7 days and 7 weeks post-surgery. **A BCCAS mice pre-surgery**. Complete circle of Willis loop (blue arrows) and absence of ECA retrograde flow (yellow arrows). **B** BCCAS 1d post-surgery. Weak MRA intensity in correspondence of ACA-MCA watershed areas (blue arrows). Retrograde flow from ECA (yellow arrows). **C**. BCCAS 7d post-surgery. Collateral flow recruitment and initial hemodynamic recovery of ACA-MCA territories inferable from an increased MRA intensity (blue arrows). **D**. BCCAS 7 weeks post-surgery. CBF recovery and return to the pre-surgery hemodynamic condition, with complete circle of Willis loop with persistence of ECA retrograde flow.

Fig S5

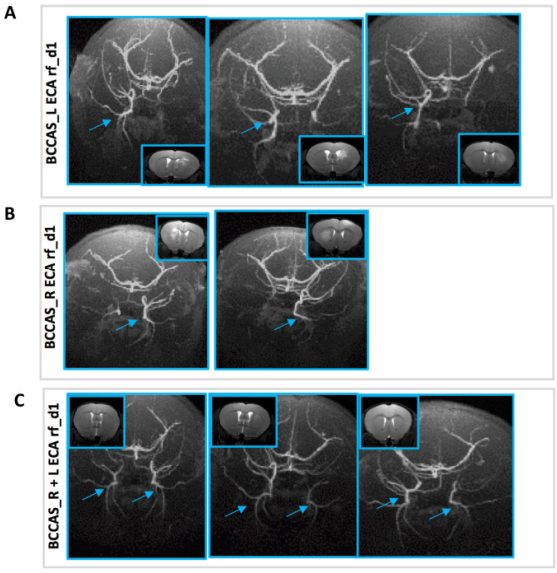

FigS5

BCCAS MRA at day 1: different pattern of ECA retrograde flow (blue arrows): only left ECA retrograde flow associated to contralateral small subcortical lesions corresponding to the right ACA-MCA border zones (**A**); only right ECA retrograde flow associated to contralateral small subcortical lesions, corresponding to the left ACA-MCA watershed areas (**B**) and both left and right ECA retrograde flow associated to no lesions detectable on T2 weighted MRI (**C**). Scale bars: B, D = 1mm; C, E= 0.5mm

Fig S6

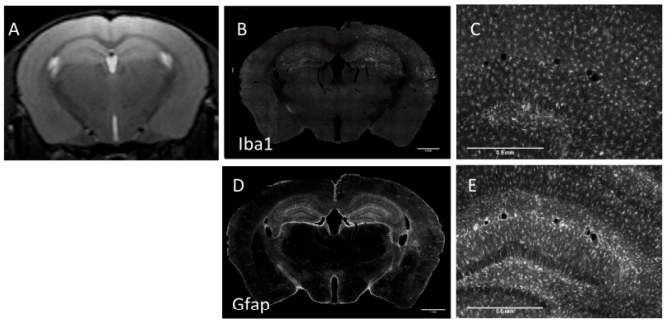

FigS6

A-E MRA (**A**), IBA1(**B-C**) and GFAP (**D-E**) staining of a BCCAS mouse displaying no ischemic lesions detectable on MRA but significant microglia and astrocytes activation in both hippocampi and right frontal cortex, 8 days post-surgery. Scale bars represent 1mm (**B**, **D**) and 0.5mm (**C**, **E**)

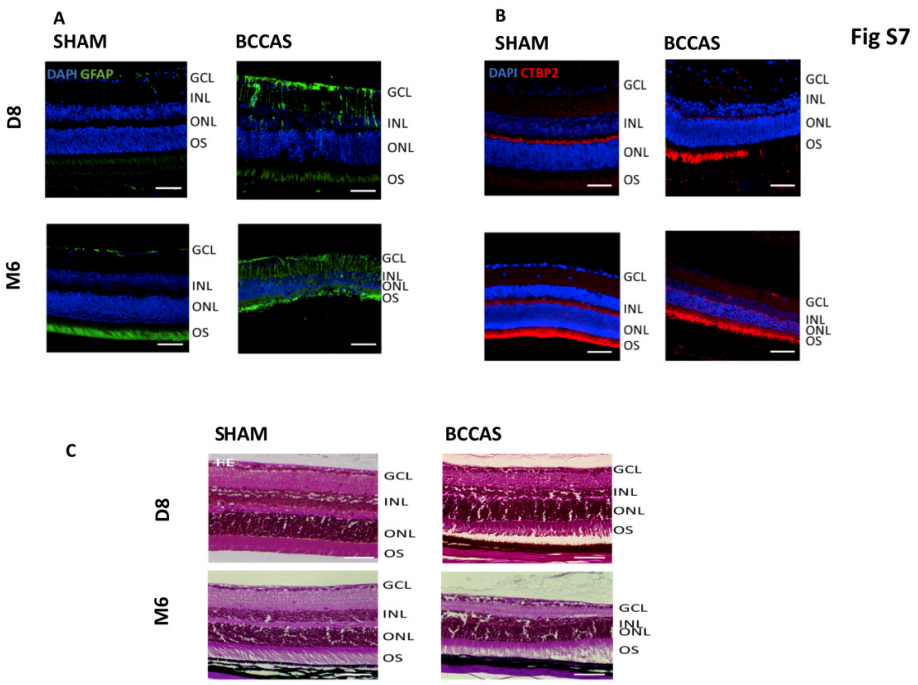

FigS7

A-C Retina progressive degeneration during subacute and chronic hypoperfusion (8 days and 6 months post-surgery, respectively) in BCCAS mice. **A**. Representative sagittal sections of the retina stained against glial fibrillary acidic protein (GFAP, in green) showing marked gliosis in BCCAS animals both at 8 days (**D8**) and 6 months (**M6**). Sham animals served as control. Nuclei are counterstained with DAPI (blue). Scale bar represents 50 um. **B**. Representative sagittal sections of the retina stained against C-terminal binding protein 2 (CTBP2, in red) showing delocalization and loss of presynaptic protein in the OPL in BCCAS animals, 8 days (**D8**), with a progressive worsening at 6 months (**M6**). Sham animals served as control. Nuclei are counterstained with DAPI (blue). Scale bar represents 50 um. **C**. Representative sagittal sections of the retina, stained with hematoxylin and eosin, displaying significant thinning and atrophy during chronic hypoperfusion (**M6**). Scale bar= 0.5mm

Fig S8

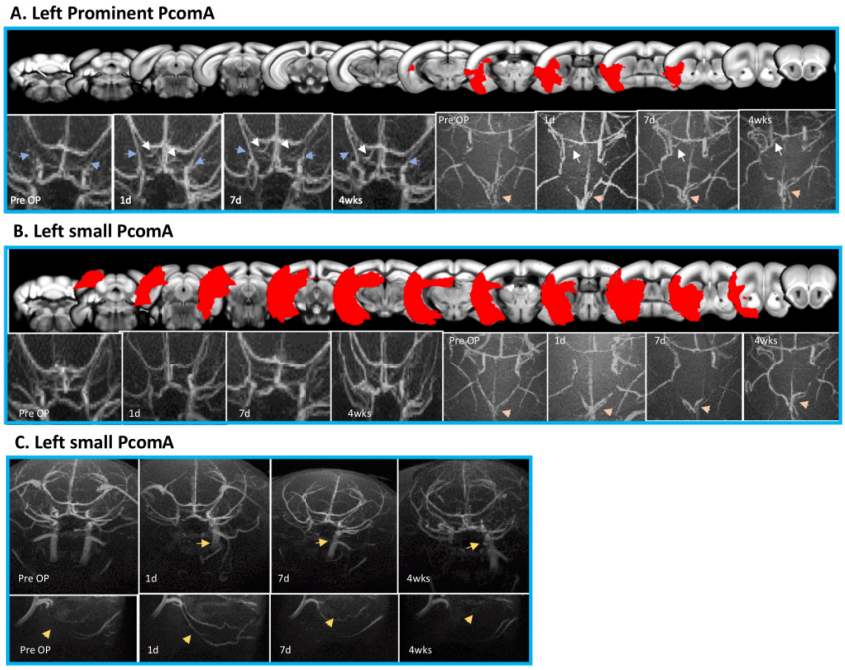

FigS8

MCAO extreme neuroimaging and vascular phenotypes: mice with prominent (**A**) and small (**B, C**) left PcomA. Detailed description in the supplementary

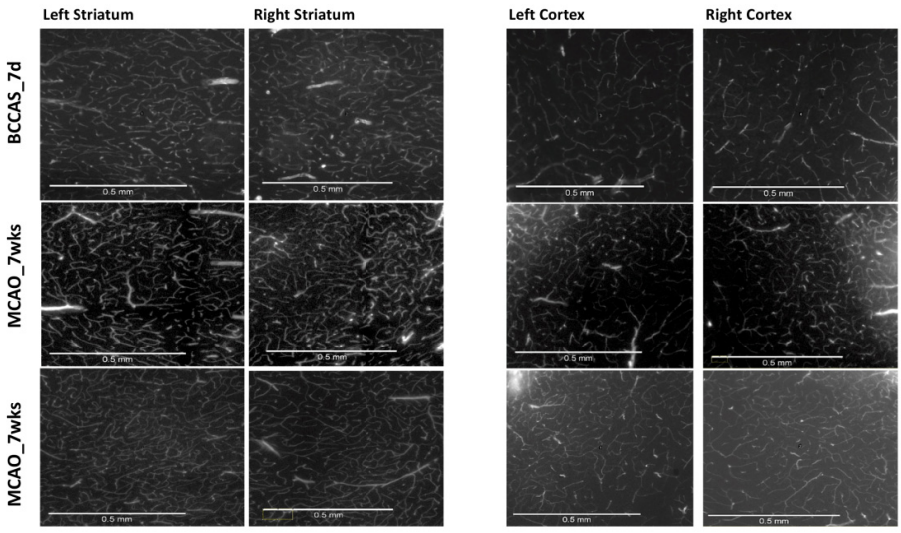

FigS9

Microllateral plasticity in hypoperfused striatum and cortex in MCAO and BCCAS mice. Scale bar represents 0.5mm

Fig S10

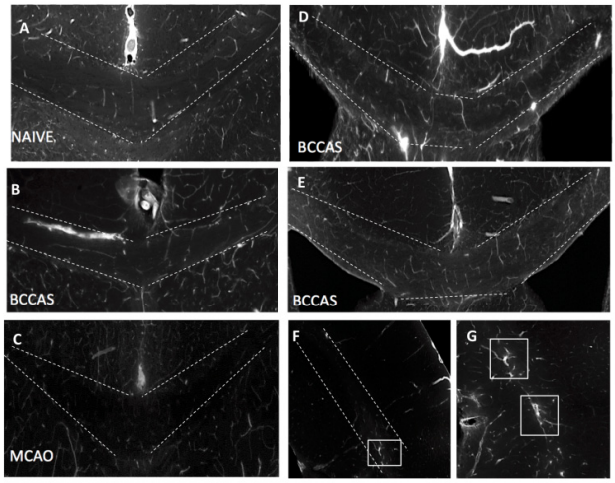

FigS10

White matter microvessels in naïve, MCAO and BCCAS mice showing a macroscopically significant reduced density of microvessels in corpus callosum (long dash lines), compared to adjacent gray matter, both for naïve, MCAO and BCCAS mice (**A-E**). Increased microvessel diameter size in white matter in proximity of the ischemic core (blue arrow) (**F, G**)

TableS1

BCCAS lesion volume and percentage of left and right hemisphere affected during acute and subacute hypoperfusion (1-7 days)

TableS2

CBF drop in BCCAS in cortex and striatum during acute and subacute hypoperfusion (1-7 days)

TableS3

Percentage of CBF reduction in BCCAS in cortex and striatum during acute and subacute hypoperfusion (1-7 days)

TableS4

Brain areas mostly affected by ischemic lesions in BCCAS at day 1

TableS5

CBF reduction in left and right hemisphere in MCAO 1 day, 1, 4 and 7 weeks post-surgery

TableS6

Percentage of CBF reduction in MCAO left and right hemisphere at day 1

TableS7

Lesion volume and percentage of left hemisphere affected at day 1 and 7 in MCAO

TableS8

Percentage of brain areas affected in MCAO mice with different PcomA patterns

TableS9

Arteriole diameter in the infarct area of MCAO mice and in naïve mice

TableS10

Microvessel features in MCAO and BCCAS hypoperfused brain areas

TableS11

Leptomeningeal vessel features in MCAO and naïve mice